Featured Article

Alternative Splicing of the *Multidrug Resistance Protein 1/ATP Binding Cassette Transporter Subfamily* Gene in Ovarian Cancer Creates Functional Splice Variants and Is Associated with Increased Expression of the Splicing Factors PTB and SRp20

Xiaolong He,[1,2] P. L. Rachel Ee,[2] John S. Coon,[3] and William T. Beck[1,2]

[1]Gynecologic Oncology Group Core Laboratory for Molecular Pharmacology and [2]Department of Biopharmaceutical Sciences, University of Illinois at Chicago, and [3]Department of Pathology, Rush University Medical Center, Chicago, Illinois

ABSTRACT

Purpose: **Overexpression of multidrug resistance protein 1 (MRP1) confers resistance to a range of chemotherapeutic agents in cell lines and could be involved in clinical drug resistance of some tumor types also. We examined MRP1 expression in a small series of untreated human ovarian tumors and matched normal tissues.**

Experimental Design: **We analyzed ten pairs of snap-frozen ovarian tumor and matched normal total ovarian tissues from the same patients for expression of MRP1 by reverse transcription-PCR. Amplified PCR products were sequenced to reveal splicing events of MRP1. MRP1 splice variants were expressed as enhanced green fluorescent fusion proteins in HEK293T cells to demonstrate their localization in the cell and their activity in conferring resistance to doxorubicin. The expression of splicing factors PTB and SRp20 was examined by Western blot.**

Results: **MRP1 was expressed in all 10 of the pairs of specimens. Multiple MRP1 cDNA fragments of various sizes were amplified between exons 10 and 19. Of interest, more MRP1 cDNA fragments were detected in ovarian tumors than in matched normal tissues in 9 of 10 pairs. We identified 10 splicing forms between exons 10 and 19 of the *MRP1* gene with exon skipping ranging from 1 to 7. Amplification of the entire coding region of MRP1 from 1 ovarian tumor revealed >20 splice variants. We found whole and partial exon skipping and partial intron inclusion in these splice variants. We expressed 3 of these MRP1 splice variants in HEK293T cells and found that they appeared to localize to the plasma membrane and were functional in conferring resistance to doxorubicin. In addition, we identified a few nucleotide variations in this gene. To understand the basis for increased splice variants in the tumors, we examined splicing factor expression in these tissues. Western blot analysis revealed that two splicing factors, PTB and SRp20, were overexpressed in most ovarian tumors compared with their matched normal ovarian tissues. Importantly, overexpression of both of these splicing factors was associated with the increased number of MRP1 splicing forms in the ovarian tissues.**

Conclusion: **The *MRP1* gene undergoes alternative splicing at a higher frequency in ovarian tumors than in matched normal tissues. Some of these splice variants confer resistance to doxorubicin. Expression of splicing factors PTB and SRp20 is strongly associated with the alternative splicing of the *MRP1* gene.**

INTRODUCTION

Ovarian cancer is the fifth most common cause of cancer-related deaths of women in the United States. Each year, >25,000 new cases are diagnosed, with ~14,000 annual deaths (1). Although considerable progress has been made in the past few decades in the diagnosis and treatment of the disease, the prognosis for overall long-term survival remains poor, with the 5-year survival ~50% (1, 2). The main obstacles to the improvement of prognosis are lack of markers for early diagnosis and resistance to chemotherapy (3). The multidrug resistance protein 1 (MRP1), originally identified from a drug-resistant lung cancer cell line, is a prototypical member of the ATP binding cassette transporter subfamily (ABCC) that has been associated with multidrug resistance (4–6). Transfection studies have demonstrated that overexpression of MRP1 in tumor cell lines can confer resistance to many natural product chemotherapeutic agents such as anthracyclines, *Vinca* alkaloid, and epipodophyllotoxins by reducing their cellular accumulation (7–9). MRP1 is ubiquitously expressed in normal tissues and can actively transport several endogenous and exogenous conjugated or unconjugated organic anions. Among endogenous substrates of MRP1 are leukotriene C4 (10), 17 R-estradiol, glutathione, glutathione disulfide (11, 12), and glucuronide- and sulfate-conjugated bile salts (13). The exogenous substrates of MRP1 include natural product and antifolate chemotherapeutic

Received 10/21/03; revised 4/11/04; accepted 4/20/04.

Grant support: National Cancer Institute Grants CA27469 to the Gynecologic Oncology Group (GOG) with subcontracts for the GOG Molecular Pharmacology Core Laboratory and the GOG Tissue Bank; CA37517 to the GOG Statistical and Data Center; CA30103 and CA40570 to W. Beck; and support from The University of Illinois at Chicago.

The costs of publication of this article were defrayed in part by the payment of page charges. This article must therefore be hereby marked *advertisement* in accordance with 18 U.S.C. Section 1734 solely to indicate this fact.

Requests for reprints: William T. Beck, Department of Biopharmaceutical Sciences (MC865), 833 South Wood Street, University of Illinois at Chicago, Chicago, IL 60612. E-mail: WTBeck@uic.edu.

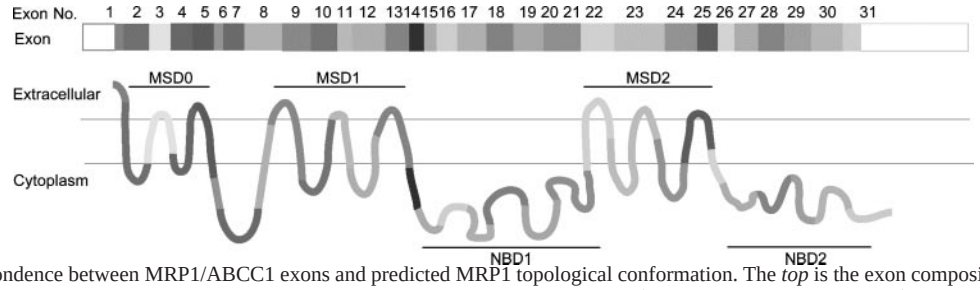

Fig. 1 Correspondence between MRP1/ABCC1 exons and predicted MRP1 topological conformation. The *top* is the exon composition of full-length MRP1. The *bottom* is the predicted topological conformation of full-length MRP1. The 5′ untranslational region and 3′ untranslational region are represented by *empty rectangles* in exons 1 and 31, respectively. The coding exons are represented by differently shaded rectangles. The topological conformation of full-length MRP1 was drawn based on the secondary structure prediction of membrane proteins by the program SOSUI.[6] The length of the rectangles and corresponding encoded peptides is approximately proportional to the length of exons.

agents, glutathione-conjugated aflatoxin B1, heavy metals, and so forth (7–9, 14). Therefore, MRP1 is thought to play an important role in elimination of metabolites and cellular detoxification. The expression of MRP1 has also been detected in many tumor tissues, including both solid and hematological malignancies (15–18). Although there are a few reports suggesting that MRP1 may be involved in the clinical drug resistance of some tumor types and of prognostic significance for response to chemotherapy in some patients (17–19), the general relevance of MRP1 expression to clinical resistance has yet to be established.

The human *MRP1* gene is located on chromosome 16 at band 13.1, spans ~194 kb, and is composed of 31 exons (20). The originally published MRP1 cDNA encodes 1531 amino acids, which is predicted to form three membrane spanning domains and two nucleotide binding domains (4–6). The correspondence of exons to the predicted MRP1 topological conformation is illustrated in Fig. 1. To date, six splice variant sequences of MRP1 besides the one mentioned above have been deposited in the National Center for Biotechnology Information RefSeq database.[4] These splice variants have exons 5, 13, 17, 18, 17, and 18, and 30 skipped, respectively. In the present study, we examined MRP1 expression in previously untreated ovarian cancers and matched normal ovarian tissues from patients with advanced epithelial ovarian cancer participating in the Gynecologic Oncology Group (GOG) Banking Protocol, GOG 136, and found that the ovarian tumors expressed more MRP1 splice variants than matched normal ovarian tissues. Importantly, the differences were associated with the expression of two splicing factors, PTB (21) and SRp20 (22). We also identified several new splice variants of the *MRP1* gene that have partial exon skipping and/or partial intron inclusion. We found that three of the splice variants, when expressed in HEK293T cells, conferred resistance to doxorubicin, but at a lower level than seen with the full-length gene.

MATERIALS AND METHODS

Specimens. Ten pairs of snap-frozen ovarian tumor and matched normal tissue were obtained from the GOG Tumor Bank (Columbus, OH). The tissue specimens were removed during primary cytoreductive surgery and before initiation of front-line chemotherapy from patients with advanced ovarian cancer who provided written consent to participate in the GOG Banking Protocol, GOG 136. The specimens were immediately snap-frozen at the GOG participating institution after surgery, shipped to the GOG Tissue Bank with dry ice, and stored at −70°C until distributed to the GOG Molecular Pharmacology Core Laboratory for testing. Of these 10 cases with paired specimens, 9 patients had a diagnosis of serous adenocarcinoma, and 1 had endometrioid carcinoma; 6 had Fédération Internationale des Gynaecologistes et Obstetristes stage III disease and 4 had Fédération Internationale des Gynaecologistes et Obstetristes stage IV disease; and 1 was a well-differentiated tumor, 7 were moderately differentiated, and 2 were poorly differentiated. In these tumor tissues, malignant cells accounted for 60–90%. The matched normal total ovarian tissues were obtained from the same patients. The specimens were labeled with coded, confidential identifiers, and the laboratory testing was performed blinded to clinical information. The use of these specimens in the study was approved by the Institutional Review Board of the University of Illinois at Chicago.

Total RNA Extraction and cDNA Synthesis. Total RNAs were extracted from 20 to 50 mg of tissue with Trizol reagent (Invitrogen, Carlsbad, CA) following the manufacturer's instruction. cDNAs were synthesized from 2 μg of total RNA with reagents contained in the ThermoScript reverse transcription-PCR system (Invitrogen). The synthesis reactions were run according to the kit manual and incubated at 55°C for 1 h.

PCR. The PCR primers for amplifying the cDNA fragments between exons 10 and 19 (primer pair 1) were 5′TGC TCT CTA CCT CCT GTG GC3′ (on exon 10) and 5′AGT AGC TCA TGC TGT GCG TG3′(on exon 19). The primers for amplifying the entire coding sequence of MRP1 (primer pair 2) were 5′GAG CTC *ATG* GCG CTC CGG GGC TTC TGC 3′ and 5′CCG CGG *CAC* CAA GCC GGC GTC TTT GGC 3′. The italicized bases are the start codon and the codon next to the stop codon, respectively. The PCR reactions were set up with the reagents contained in ThermoScript reverse transcription-PCR system (Invitrogen) except that High Fidelity Platinum TaqDNA polymerase was used instead of Platinum Taq to amplify the entire coding sequences. The cycling conditions were 95°C for 2 min, then 40 cycles of 94°C for 20 s, 60°C for

[4] Internet address: http://www.ncbi.nlm.nih.gov/sutils/evv.cgi?contig=NT_010393.13&gene=ABCC1&lid=4363.
[6] Internet address: http://sosui.proteome.bio.tuat.ac.jp/sosuimenu0.html.

20 s, 72°C for 1.5 min followed by 1 cycle of 72°C for 10 min. The extension condition was 68°C for 5 min when the entire coding sequences were amplified.

DNA Sequencing. PCR products were first cloned into TOPO TA cloning vector (Invitrogen) by following the kit manual. The bacterial colonies obtained were randomly picked and examined by colony PCR to estimate the insert sizes. Colonies carrying different size inserts were selected for plasmid preparation, and the resulting plasmids were submitted for automatic sequencing. Several internal primers were used when the entire coding region of MRP1 was sequenced.

Western Blot. Ten mg to 20 mg of tissue specimens were homogenized with Kontes ground glass tissue grinder in 100–200 μl T-PER Tissue Protein Extraction Reagent (Pierce Biotechnology, Rockford, IL) supplemented with protease inhibitor mixture [2 mM 4-(2-aminoethyl) benzenesulfonylfluoride, 1 mM EDTA, 130 μM bestatin, 14 μM L-*trans*-3-carboxyoxiran-2-carbonyl-L-leucylagmatine *N*-(*trans*-epoxysuccinyl)-L-leucine 4-guanidinobutylamide *trans*-epoxysuccinyl-L-leucylamido(4-guanidino)butane, 1 mM leupeptin, and 0.3 μM aprotinin; Sigma, St. Louis, MO]. The homogenates were then centrifuged at 10,000 rpm at 4°C for 5 min to remove cell/tissue debris. Supernatants (20 μl) from each specimen were applied to SDS-PAGE on a 4–20% gradient gel, and proteins were transferred to a nitrocellulose membrane using a semidry electroblotter. The blot was then blocked in 5% milk and probed with monoclonal antibody PTB (Ab-1; Oncogene Research Products, San Diego, CA) and SRp20 (7B4; Santa Cruz Biotechnology, Santa Cruz, CA), followed by horseradish peroxidase-conjugated donkey antimouse IgG. Signals were detected with enhanced chemiluminescence Western blotting detection reagents (Amersham Pharmacia Biotech, Piscataway, NJ).

Construction of Expression Vectors and Transfection. cDNAs of MRP1 splice variants amplified as above were subcloned into pDsRed1-N1 (Clontech, Palo Alto, CA) between sites *Sac*I and *Sal*I. The DsRed1 coding sequence was then replaced by the enhanced green fluorescent protein coding sequence. Therefore, enhanced green fluorescent protein was fused to the COOH termini of the MRP1 variants. The expression vectors were introduced into HEK293T cells by calcium-phosphate precipitation. Transfection efficiency ranged from 30 to 80%.

Chemosensitivity Assay. The drug sensitivity of cells was determined using the colorimetric 3-(4,5-dimethylthiazol-2-yl)-2,5-diphenyltetrazolium bromide assay basically as described previously (23). Briefly, HEK293T cells transfected for 24 h were seeded at 5×10^3 cells/well in 100 μl of culture medium in 96-well plates. The following day, serially diluted doxorubicin (Sigma) in culture medium was added to cells (100 μl/well) in triplicate. Seventy-two h later, 100 μl of medium was removed from each well, and the 3-(4,5-dimethylthiazol-2-yl)-2,5-diphenyltetrazolium bromide reagent (25 μl/well, 2 mg/ml; Sigma) was added. After incubation at 37°C for 3 h, the medium was carefully removed from each well, and 100 μl of DMSO was added to solubilize the formazan. Color density was determined using the microplate reader (Molecular Devices, Sunnyvale CA). Mean values (± SD) of three independent experiments were plotted using SigmaPlot package (SPSS Inc., Chicago, IL).

Fluorescence Microscopy. HEK293T cells were seeded on gelatin-coated coverslips in 12-well plates at 1×10^5 cells per well 24 h before transfection. Twenty-four h after transfection, the coverslips were washed once with PBS and then fixed with 2% paraformaldehyde in PBS for 20 min at room temperature. After washing twice with PBS, the cells were permeabilized in 0.2% Triton X-100 in PBS for 30 min and then incubated in 0.5 ml RNAase A (10 μg/ml in 0.1% Triton X-100/1% BSA in PBS) for 60 min at room temperature. After washing once with PBS, the cell nuclei were stained by incubation in 0.5 ml of propidium iodide (2 μg/ml in PBS; Sigma) for 45 min in the dark. Finally, the coverslips were mounted on slides with 1 drop of Antifade Solution (Molecular Probes, Eugene, OR), and the cells were examined under Axiotron 2 laser scanning microscope (Carl Zeiss, Thornwood, NY).

Statistical Analysis. SPSS version 10.0 (SPSS Inc., Chicago, IL) was used for the data analysis. A paired-samples *t* test was used to test the hypotheses of no difference between the number of MRP1 splicing variants detected in tumor and matched normal tissue.

RESULTS

Ovarian Tumor Tissues Express, on Average, More MRP1 Splice Variants Than Matched Normal Tissues. Our previous study showed that both ovarian tumors and their matched normal tissues expressed MRP1, and there was no significant difference between them.[5] To examine whether ovarian tumors and their matched normal total ovarian tissues express MRP1 splice variants differently, we designed five primer pairs to amplify five overlapping MRP1 cDNA fragments spanning from exon 3 to exon 31 from 10 pairs of matched tumor and normal ovarian tissues. These five primer pairs are located on exons 3 and 11, exons 10 and 19, exons 18 and 24, exons 23 and 31, and exons 29 and 31, respectively. The result of amplifications with primer pair located on exons 10 and 19 is shown in Fig. 2*A*. It can be seen that more than one product was amplified from 18 specimens of 20 total. The size of the major product is ~1.15 kb, which is consistent with the expected size, 1136 bp, of the cDNA fragment containing all of the exons between exon 10 and exon 19 of MRP1, according to RefSeq NM_004996. Of most interest, more PCR products of different sizes were amplified from 9 tumor specimens than from their matched normal tissues (pairs 2–10). Only in 1 pair (pair 1) did it appear that more PCR products of different sizes were seen in normal tissue compared with tumor. On the agarose gel, 3–12 PCR product bands can be recognized from tumor tissues (Fig. 2*A*). As summarized in Table 1, counting the numbers of different PCR products in each specimen, it is seen that there are 7 cases with 2–10 times more PCR product bands in tumors than in matched normal tissues. The amplification of MRP1 cDNA fragments between exon 18 and exon 24, exon 23 and exon 31, and exon 29 and exon 31 produced only 1 band in most specimens (data not shown). The amplification of MRP1 cDNA fragments between exon 3 and exon 11 failed in most speci-

[5] X. He and W. T. Beck, unpublished observations.

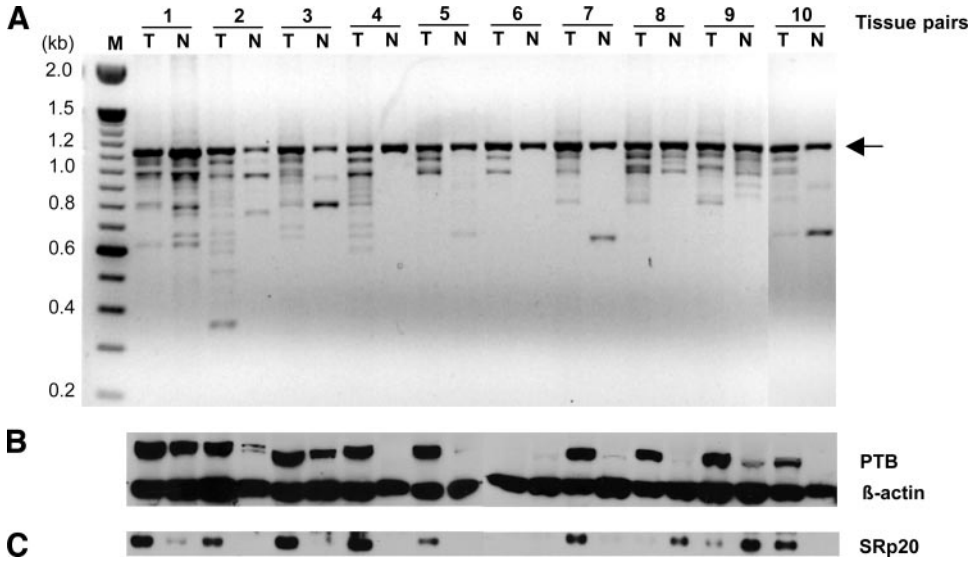

Fig. 2 *A*, agarose gel electrophoresis of PCR-amplified MRP1 cDNA fragments between exon 10 and exon 19 from 10 pairs of matched tumor and normal ovarian tissues. The *arrow on the right* indicates PCR products of the size expected based on RefSeq NM_004996. *T*, tumor; *N*, Normal. *B* and *C*, Western blot analysis of PTB and SRp20 expressions, respectively, in these 10 pairs of tissues. See "Materials and Methods" for details.

mens. This was probably due to the difficulty in cDNA synthesis to reach to the very 5′ end.

Splicing Forms between Exons 10 and 19 of MRP1. To verify that the PCR amplifications of multiple DNA bands described above are specific to the *MRP1* gene, PCR products from tumor tissue of pair 2 were cloned into the TOPO TA cloning vector and clones of various sizes of inserts were selected for sequencing. Alignment of obtained sequences with RefSeq NM_004996 reveals that they are all MRP1-specific and result from alternative splicing of MRP1 pre-mRNA. To date, we have identified 10 splicing forms between exon 10 and exon 19 including the 1 containing all of the exons in this region (Fig. 3). They are all alternatively spliced at the exon/intron boundary consensus sites. The number of skipped exons ranges from 1 to 7. Of these 10 splicing forms, 7 (splicing forms 3, 4, and 6–10) are new compared with the MRP1/ABCC1 splice variants in the National Center for Biotechnology Information databases. By carefully comparing the size of the PCR products amplified from all of the tissues shown in Fig. 3, we conclude that the MRP1 splicing forms in this region are far beyond 10.

MRP1 Splice Variants Include Partial Exon Skipping and Partial Intron Inclusion. We also amplified the entire coding sequences of MRP1 from the ovarian tumor tissue of pair 4. The PCR result is shown in Fig. 4*A*. On the agarose gel, we can see 2 major DNA bands, one ~4.3 kb and the other between 2.0 and 2.3 kb. We gel-purified these 2 DNA bands and cloned them into TOPO TA cloning vector. *Pst*I digestion of the obtained plasmids revealed >20 digestion patterns. This indicates that the DNA band ~4.3 kb in Fig. 4*A* is actually a complex of DNA molecules of many different sizes. Fig. 4*C* shows the result of *Pst*I digestion of some plasmids. According to the sequence of RefSeq NM_004996, there are five *Pst*I sites within the coding region of MRP1 cDNA (Fig. 4*B*). *Pst*I digestion gives rise to three visible DNA fragments of sizes 1.1 kb, 1.6 kb, and 1.7 kb, as well as two very small DNA fragments of sizes 72 bases and <50 bases, respectively (Fig. 4*B*). We have analyzed 16 MRP1 splice variants by DNA sequencing and found that these splice variants exhibited partial exon skipping and/or partial intron inclusion as well as whole exon skipping(s). The smallest variant identified is only 2.2 kb, and exons 12–26 and part of exon 27 were skipped. Table 2 lists the details of splicing events that occurred in these variants. Among them, 11 are novel and are not found in the literature or National Center for Biotechnology Information databases.

Nucleotide Variations in the MRP1 Coding Sequence. Apart from different splicings, sequencing analysis of MRP1 splice variants discussed above (Table 2) also revealed a few nucleotide variations compared with RefSeq NM_004996 (Table 3). These variations were found in all of the splice variants listed in Table 2 as well as in the genomic DNA of the matched normal ovarian tissue. Therefore, they represent polymorphisms of the *MRP1/ABCC1* gene instead of somatic mutations. None of these variations caused any amino acid substitutions.

Table 1 Number of DNA bands amplified between exon 10 and exon 19

The number of DNA bands were quantified from the photo of agarose gel after electrophoresis (Fig. 2*A*) with the assistance of Adobe Photoshop. The paired-samples *t* test procedure was performed to compare the number of MRP1 splicing variants observed in tumor and matched normal tissue ($P = 0.007$).

Tissue pair	Tumor	Normal
Pair 1	9	11
Pair 2	12	4
Pair 3	10	3
Pair 4	10	1
Pair 5	4	2
Pair 6	3	1
Pair 7	5	2
Pair 8	7	4
Pair 9	7	6
Pair 10	8	3
Total	75	37
Average	7.5	3.7

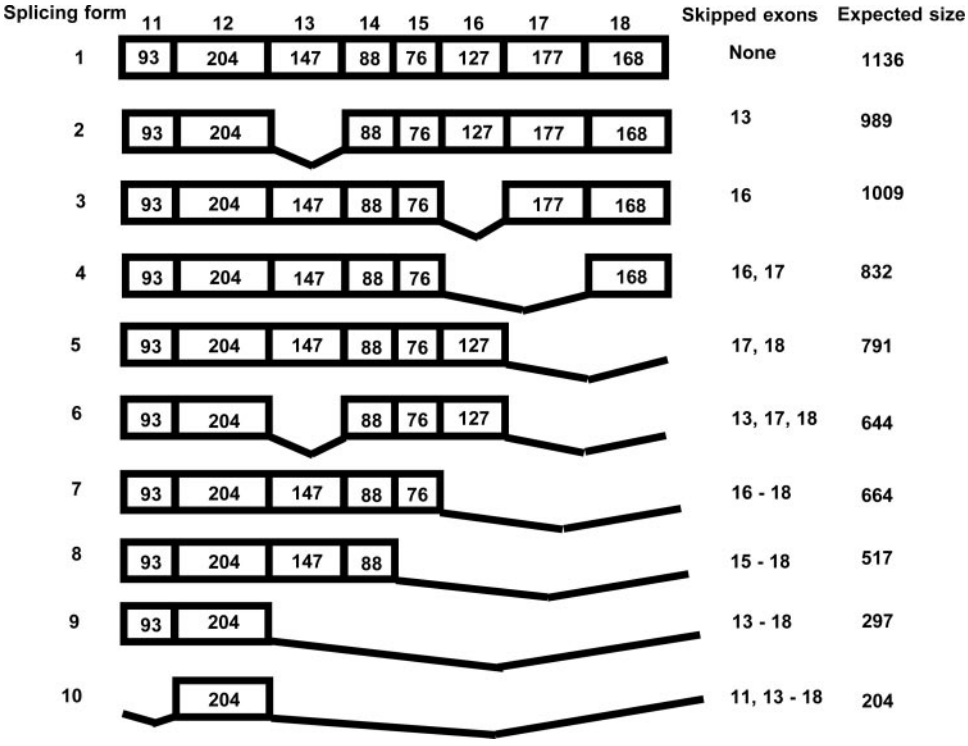

Fig. 3 Schematic diagrams of splicing forms of MRP1 between exon 10 and exon 19 identified in the tumor tissue of pair 2. The numbers on the *top* indicate the exons between exon 10 and exon 19. Exons are represented by □. The *number in each rectangle* indicates the size (bp) of the corresponding exon. Exon 10 and exon 19 have 21 and 34 bases included in the PCR products, respectively, but these are not shown in the figure. The skipped exons are left blank.

Splicing Factors PTB and SRp20 Are Overexpressed in Ovarian Tumors. The process of pre-mRNA splicing is regulated by a variety of splicing factors. Changes in the expression and distribution of splicing factors are often the causes of alterations in splicing patterns (24). Accordingly, our observation described above could be a consequence of changes in splicing factors. Thus, we examined by Western blot the expression of two splicing factors, PTB (Fig. 2*B*) and SRp20 (Fig. 2*C*), in the 10 pairs of matched tumor and normal ovarian tissues. PTB and SRp20 are negative and positive regulators of pre-mRNA splicing, respectively (25). Fig. 2*B* indicates that the expression of PTB is up-regulated in 8 of 10 tumors compared with their matched normal tissues (pairs 2–5 and 7–10). Of interest, the overexpression of PTB is accompanied by more MRP1 splicing forms between exon 10 and exon 19 (Fig. 2, *A* and *B*). In pair 1, both tumor and normal tissues highly express PTB; they also both express more MRP1 splicing forms. In 8 tissue pairs, PTB is overexpressed in tumors, and more MRP1 splicing forms are also seen in these tumors. Fig. 2*C* reveals that SRp20 is up-regulated in 7 of 10 tumors compared with their

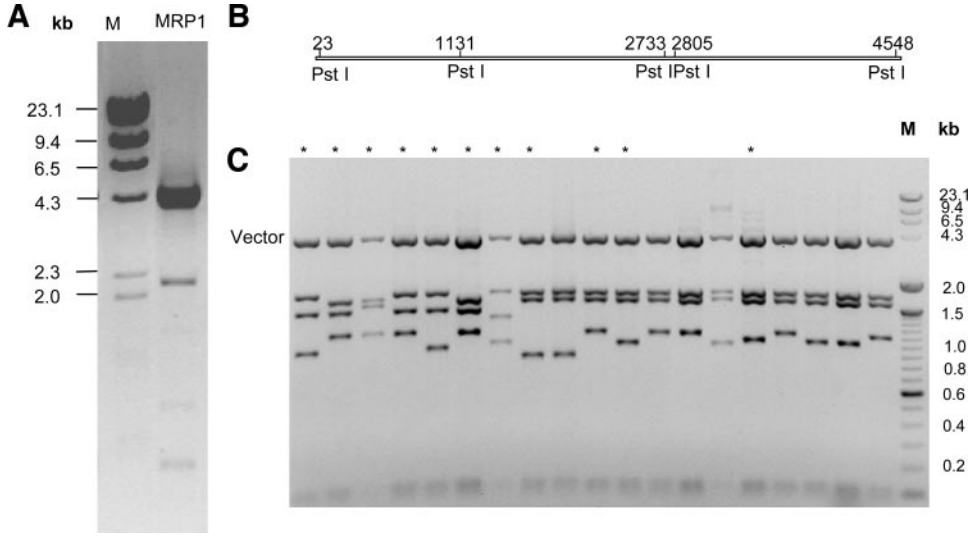

Fig. 4 A, reverse transcription-PCR of the entire coding sequences of MRP1 from the tumor tissue of pair 4. *B, Pst*I sites in the coding sequence of NCBI RefSeq NM_004996. The number is relative to the start codon. The size of the coding sequence of NM_004996 is 4593 nucleotides. *C, Pst*I digestion of plasmids carrying entire coding sequences of some MRP1 splice variants. ∗ marks the clones of different digestion pattern. The *unmarked lanes* have digestion patterns same as one of the *marked lanes*.

Table 2 MRP1 variants identified from one ovarian tumor tissue[a]

MRP1 variants	Size (kb) of coding	Skipped exons	Included introns	Frame shift
MRP1	4.6	No	No	No
MRP1–2k[b]	2.2	Exons 12–26, 99 nucleotides of exon 27 in 3′ portion	No	No
MRP1-d5	4.5	Exon 5	No	No
MRP1-d13	4.4	Exon 13	No	No
MRP1-d17	4.4	Exon 17	No	No
MRP1-d4d5[b]	4.3	Exons 4 and 5	No	No
MRP1-d16d17[b]	4.3	Exons 16 and 17	No	Yes, premature stop
MRP1-d17d18	4.2	Exons 17 and 18	No	No
MRP1-d17d25[b]	4.3	Exons 17 and 25	No	Yes, premature stop
MRP1-d5d30[b]	4.3	Exons 5 and 30	No	No
MRP1-v9[b]	4.1	Exons 13, 17 and 18	No	No
MRP1-d2d17[b]	4.2	Exons 2 and 17	No	No
MRP1-d18d25[b]	4.3	97 nucleotides of exon 18 in 5′ portion and exon 25	No	Yes, premature stop
MRP1-v6[b]	4.8	No	193 nucleotides of intron 6, 118 nucleotides downstream of exon 6	Yes, premature stop
MRP1-v10[b]	4.6	Exon 13	193 nucleotides of intron 6, 118 nucleotides downstream of exon 6	Yes, premature stop
MRP1-v5[b]	4.5	88 nucleotides of exon 5 in 5′ portion	No	Yes, premature stop

[a] Sequences of MRP1 splice variants were analyzed with bioinformatics tools at http://workbench.sdsc.edu.
[b] Novel MRP1 splice variants.

matched normal tissues (pairs 1–5, 7, and 10), and 6 of these also have more MRP1 splicing forms in tumors relative to the matched normal tissue. PTB and SRp20 are, however, not detected in the tumor or the normal tissue in pair 6, yet 3 distinct MRP1 splicing forms are observed in the tumor compared with the 1 MRP1 splicing form detected in the matched normal tissue, suggesting that other splicing factors may also play a role in generating splice variants in some tumors.

Expressing MRP1 Splice Variants in HEK293T Cells. Because of the increased number of MRP1 splice variants in most of the tumors, we wished to know if these splice variants produce any phenotypes. To study the function and localization of MRP1 splice variants in the cell, we constructed expression vectors of three MRP1splice variants, MRP1–2k, MRP1-d5d30, and MRP1-d17d18, as well as full-length MRP1, all with enhanced green fluorescent protein fused to their COOH termini, and we expressed these fusion proteins in HEK293T cells. The expression and localization of these splice variants in HEK293T cells are shown in Fig. 5. It can be seen that expression of these variants, like the full-length MRP1, appears to localize mainly on the plasma membrane.

MRP1 Splice Variants Can Confer Drug Resistance on HEK293T. To determine whether the MRP1 splice variants are functional, we examined the resistance to doxorubicin of HEK293T cells transfected by the above expression vectors. This chemotherapeutic agent can be actively transported by full-length human MRP1 (9). The chemosensitivity of transfected HEK293T was determined by colorimetric 3-(4,5-dimethylthiazol-2-yl)-2,5-diphenyltetrazolium bromide assays after exposure to serial dilutions of doxorubicin. The results are shown in Fig. 6 and are summarized as relative resistance factors in Table 4. It is clear that the three MRP1 splice variants conferred drug resistance on HEK293T cells, although they were not as potent as the full-length MRP1. The large SDs in relative resistance factors are probably due to the variable transfection efficiencies from one experiment to another.

DISCUSSION

After transcription, cells undergo a series of RNA processing reactions before active proteins can be produced. Among RNA processing events, pre-mRNA splicing, which is catalyzed by a large molecular complex called the spliceosome, is probably the most complicated (25, 26). Through splicing, intervening sequences (introns) that disrupt the exonic sequences (exons) are removed from pre-mRNA, and exons are joined together to form a mRNA molecule. For many genes, their exons are not always all included in the mature mRNAs. Rather, some exons undergo alternative splicing, and their inclusion is regulated by a variety of internal and external signals (24). Genome-wide analyses revealed that 40–60% of human genes

Table 3 Nucleotide variations of MRP1 mRNA

Nucleotide variations were identified by aligning sequences of MRP1 splice variants in Table 2 to RefSeq NM_004996. The nucleotide substitutions were found in all of the MRP1 splice variants listed in Table 2 as well as in the genomic DNA of the matched normal ovarian tissue. The position of nucleotide refers to that as described in NM_004996.

Position	Nucleotide variation
546	C→T
1021	T→C
1258	T→C
1880	T→C

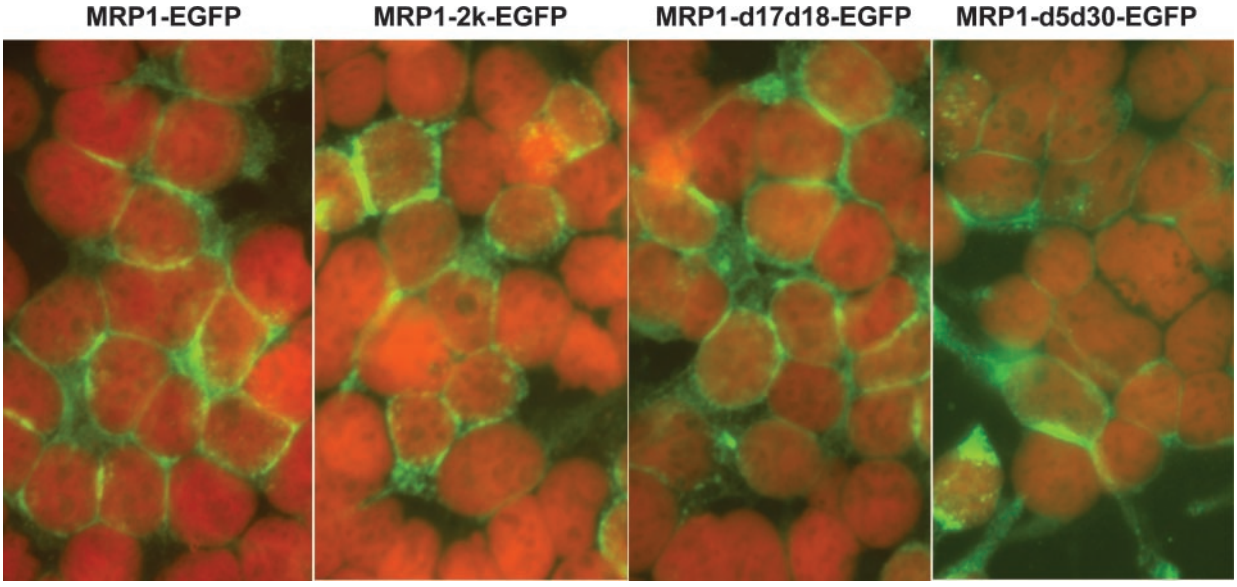

Fig. 5 Fluorescence microscopy of HEK293T cells transfected by expression vectors of full-length MRP1 or three MRP1 splice variants with enhanced green fluorescent protein (*EGFP*) fused to their COOH termini. The localization of full-length MRP1 or MRP1 splice variants is indicated in *green*. Nuclei stained by propidium iodide are shown in *red*.

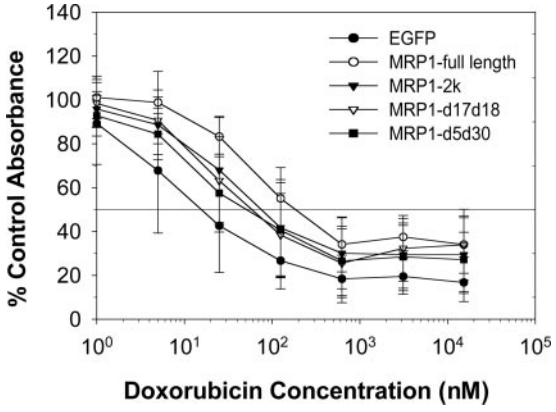

Fig. 6 3-(4,5-Dimethylthiazol-2-yl)-2,5-diphenyltetrazolium bromide assay of doxorubicin cytotoxicity to HEK293T cells transfected by expression vector of full-length MRP1 or three MRP1 splice variants with enhanced green fluorescent protein (*EGFP*) fused to their COOH termini, respectively, or EGFP only. See "Materials and Methods" for details; *bars*, ±SD.

undergo alternative splicing (27). The importance of alternative splicing is manifested not only by its role of increasing proteomic complexity in the body but also by its connections to many human diseases, including cancers (28, 29). In our study, we observed, in a small series of paired tissue specimens from previously untreated patients with Fédération Internationale des Gynaecologistes et Obstetristes stage III or IV epithelial ovarian carcinoma, that ovarian tumors expressed on average ~2-fold more MRP1 splice variants than matched normal tissues. The splicing events that occurred in the *MRP1* gene in these tumors included partial exon skipping, partial intron inclusion, and whole exon skipping. The number of skipped exons in this gene can be as many as 15. Moreover, our data demonstrate clearly that MRP1 splice variants have phenotype, because they are functional in conferring drug resistance in HEK293T cells.

Alterations in pre-mRNA splicing have been found in several tumors. One of the most studied is that between CD44 gene splicing and tumor progression and metastasis. Breast, ovary, and colon cancers highly express alternatively spliced CD44 variants, whereas normal tissues mainly express the standard version of CD44 (30, 31). Overexpression of the CD44 splice variant CD44v6 conferred metastatic potential to a non-metastatic cell line, and the CD44 splicing pattern was also shown to change during mammary tumorigenesis (32). Our novel observation that ovarian tumors express on average twice as many MRP1 splice variants is another example of an association between cancer and gene splicing pattern changes. Given the demonstration in this study that MRP1 splice variants are functional, we postulate that mis-splicing of the *MRP1* gene might be involved in tumorigenesis and the progression of

Table 4 Relative drug resistance of HEK293T cells transfected with MRP1 and its splice variants

Relative resistance factor was obtained by dividing the IC_{50} of full-length MRP1-EGFP or MRP1 splice variants-EGFP fusion protein-transfected cells by the IC_{50} of EGFP only-transfected cells. The values shown represent the mean ± SD determined from three independent experiments.

Transfection	Relative resistance factor
EGFP[a] only	1
Full-length MRP1-EGFP	6.9 ± 2.5
MRP1-2k-EGFP	4.2 ± 2.4
MRP1-d17d18-EGFP	3.6 ± 2.7
MRP1-d5d30-EGFP	3.7 ± 3.9

[a] EGFP, enhanced green fluorescent protein.

ovarian cancer and could influence the response of these tumors to chemotherapeutic treatment. However, it seems unlikely that aberrances in pre-mRNA splicing can trigger the oncogenic process. We are presently investigating whether MRP1 splice variants have functions other than conferring drug resistance, and we are considering the possibility of using mis-spliced MRP1 variants as markers for diagnosis and prognosis of cancer or drug responsiveness.

The possible causes resulting in more splice variants in ovarian tumors compared with their matched normal tissues are likely due to sequence mutations, alterations in splicing machinery, or both. In this study, we found that two splicing factors, PTB and SRp20, are overexpressed in most ovarian tumors compared with their matched normal tissues. Moreover, the overexpression of PTB and SRp20 are both associated with more MRP1 splice variants (Fig. 1). PTB, also known as heterogeneous nuclear ribonucleoprotein I, was first identified as a polypeptide that bound the U-rich polypyrimidine tracts that typically precede the 3′ splice site of introns (21). As a splicing factor, PTB has been shown to repress exon inclusion in a number of genes and, thus, induce exon skipping. Genes regulated negatively by PTB in pre-mRNA splicing include α- and β-*tropomyosin* (33–35), *FGF-R1* (36), *FGF-R2* (37, 38), *c-src* (39), *GABAγ2* (40), *fibronectin* (41), *caspase-2* (42), and α-*actinin* (43). Our results suggest that the *MRP1* gene could be another target regulated by PTB. The exon skipping events between exons 10 and 19 of MRP1 in ovarian tumors are very likely a consequence of the overexpression of PTB, but additional study is required to elucidate the detailed mechanism behind the phenomenon.

SRp20 is a member of the SR protein family, which is characterized by high serine (S) and arginine (R) content and extensive repetition of the R-S dipeptide in the COOH terminus. SR proteins are essential multifunctional splicing factors required at different steps of spliceosome assembly (22). They promote exon recognition by binding to the exon splicing enhancers and recruiting other general splicing factors to the pre-mRNAs (22, 25). Thus, in contrast to PTB, SR proteins are regarded as positive regulators of pre-mRNA splicing. Overexpression of SRp20 observed in most ovarian tumors in this study could cause more splicing forms of MRP1 by promoting the recognition of weak exons located in introns. Indeed, a partial intron is included in some MRP1 splice variants isolated from one ovarian tumor examined (Table 2). We are presently attempting to determine whether there is a direct connection between SRp20 overexpression and changes in MRP1 splicing.

Besides *trans*-acting factors, *cis*-elements are other important factors in determining the accuracy of pre-mRNA splicing. The *cis*-elements include 5′ and 3′ splicing sites, branch points, and short sequences called splicing enhancers and silencers within or near the exon (25, 44). Nucleotide changes in these elements have been shown to cause defects in pre-mRNA splicing and lead either directly to disease or to predisposition to disease (29). Among the nucleotide variations of MRP1 found in the present study, the substitution at position 546 is located at the 5′ splicing site of exon 3 of MRP1, and other substitutions are located at nucleotides 16, 22, and 7 from the 3′ splicing site of exons 8, 9, and 13, respectively. Whether these variations contributed to the splicing pattern changes in ovarian tumors remains to be clarified.

Because most ovarian tumors arise from ovarian surface epithelium (45), and the content of epithelial cells in normal ovarian tissues is usually less than in ovarian tumors, we need to compare the splicing pattern of MRP1 and expression of splicing factors in isolated normal ovarian epithelial cells with that of epithelial ovarian tumors to additionally confirm our observations described above and study the possible roles of MRP1 splice variants and splicing factors in tumorigenesis and tumor progression. In addition, it is possible that different types of cells express different sets of MRP1 splice variants. To study the distribution of individual MRP1 splice variants in the tissues, it is necessary to develop antibodies to recognize the peptides encoded by exon-exon junction sequences.

In summary, we observed more MRP1 splice variants in ovarian tumors than in matched normal tissues and found that these splice variants conferred a drug resistance phenotype. Correspondingly, we found that splicing factors PTB and SRp20 are overexpressed in most tumors compared with their matched normal tissues. Our observations suggest that alternative/aberrant splicing is a common feature in advanced epithelial ovarian carcinoma. The relationships among these MRP1 splicing variants and splicing factors, their role(s) in tumorigenesis, and the progression and therapy response of ovarian cancer (and possibly other tumors) merit additional investigation.

ACKNOWLEDGMENTS

We thank our colleagues at the Gynecologic Oncology Group (GOG) and the GOG Tumor Bank for providing the frozen tissue specimens for this translational research study. We thank Dr. Yin-Yuan Mo (University of Illinois at Chicago; UIC) for helpful discussion, and we are grateful to Martina Vaskova (UIC) for outstanding administrative support. We thank Dr. Teresa Orenic (UIC) for assistance in using the laser scanning microscope and we are most grateful to Dr. Kathleen Darcy of the GOG Statistical and Data Center for statistical analysis and editorial help.

REFERENCES

1. Jemal A, Murray T, Samuels A, Ghafoor A, Ward E, Thun MJ. Cancer statistics, 2003. CA Cancer J Clin 2003;53:5–26.

2. Harries M, Gore M. Part I: chemotherapy for epithelial ovarian cancer-treatment at first diagnosis. Lancet Oncol 2002;3:529–36.

3. Herbst AL. The epidemiology of ovarian carcinoma and the current status of tumor markers to detect disease. Am J Obstet Gynecol 1994; 170:1099–105; discussion 1105–7.

4. Cole SP, Bhardwaj G, Gerlach JH, et al. Overexpression of a transporter gene in a multidrug-resistant human lung cancer cell line. Science 1992;258:1650–4.

5. Zaman GJ, Versantvoort CH, Smit JJ, et al. Analysis of the expression of MRP, the gene for a new putative transmembrane drug transporter, in human multidrug resistant lung cancer cell lines. Cancer Res 1993;53:1747–50.

6. Schneider E, Horton JK, Yang CH, Nakagawa M, Cowan KH. Multidrug resistance-associated protein gene overexpression and reduced drug sensitivity of topoisomerase II in a human breast carcinoma MCF7 cell line selected for etoposide resistance. Cancer Res 1994;54: 152–8.

7. Zaman GJ, Flens MJ, van Leusden MR, et al. The human multidrug resistance-associated protein MRP is a plasma membrane drug-efflux pump. Proc Natl Acad Sci USA 1994;91:8822–6.

8. Grant CE, Valdimarsson G, Hipfner DR, Almquist KC, Cole SP, Deeley RG. Overexpression of multidrug resistance-associated protein (MRP) increases resistance to natural product drugs. Cancer Res 1994; 54:357–61.

9. Cole SP, Sparks KE, Fraser K, et al. Pharmacological characterization of multidrug resistant MRP-transfected human tumor cells. Cancer Res 1994;54:5902–10.

10. Leier I, Jedlitschky G, Buchholz U, Cole SP, Deeley RG, Keppler D. The MRP gene encodes an ATP-dependent export pump for leukotriene C4 and structurally related conjugates. J Biol Chem 1994;269: 27807–10.

11. Leier I, Jedlitschky G, Buchholz U, et al. ATP-dependent glutathione disulphide transport mediated by the MRP gene-encoded conjugate export pump. Biochem J 1996;314:433–7.

12. Heijn M, Hooijberg JH, Scheffer GL, Szabo G, Westerhoff HV, Lankelma J. Anthracyclines modulate multidrug resistance protein (MRP) mediated organic anion transport. Biochim Biophys Acta 1997; 1326:12–22.

13. Jedlitschky G, Leier I, Buchholz U, Barnouin K, Kurz G, Keppler D. Transport of glutathione, glucuronate, and sulfate conjugates by the MRP gene-encoded conjugate export pump. Cancer Res 1996;56: 988–94.

14. Loe DW, Stewart RK, Massey TE, Deeley RG, Cole SP. ATP-dependent transport of aflatoxin B1 and its glutathione conjugates by the product of the multidrug resistance protein (MRP) gene. Mol Pharmacol 1997;51:1034–41.

15. Chauncey TR. Drug resistance mechanisms in acute leukemia. Curr Opin Oncol 2001;13:21–6.

16. Ota E, Abe Y, Oshika Y, et al. Expression of the multidrug resistance-associated protein (MRP) gene in non-small-cell lung cancer. Br J Cancer 1995;72:550–4.

17. Nooter K, Brutel de la Riviere G, Look MP, et al. The prognostic significance of expression of the multidrug resistance-associated protein (MRP) in primary breast cancer. Br J Cancer 1997;76:486–93.

18. Endo K, Maehara Y, Ichiyoshi Y, et al. Multidrug resistance-associated protein expression in clinical gastric carcinoma. Cancer 1996;77:1681–7.

19. Norris MD, Bordow SB, Marshall GM, Haber PS, Cohn SL, Haber M. Expression of the gene for multidrug-resistance-associated protein and outcome in patients with neuroblastoma. N Engl J Med 1996;334: 231–8.

20. Grant CE, Kurz EU, Cole SP, Deeley RG. Analysis of the intron-exon organization of the human multidrug-resistance protein gene (MRP) and alternative splicing of its mRNA. Genomics 1997;45: 368–78.

21. Garcia-Blanco MA, Jamison SF, Sharp PA. Identification and purification of a 62,000-dalton protein that binds specifically to the polypyrimidine tract of introns. Genes Dev 1989;3:1874–86.

22. Graveley BR. Sorting out the complexity of SR protein functions. Rna 2000;6:1197–211.

23. Zhang DW, Cole SP, Deeley RG. Identification of an amino acid residue in multidrug resistance protein 1 critical for conferring resistance to anthracyclines. J Biol Chem 2001;276:13231–9.

24. Stamm S. Signals and their transduction pathways regulating alternative splicing: a new dimension of the human genome. Hum Mol Genet 2002;11:2409–16.

25. Maniatis T, Tasic B. Alternative pre-mRNA splicing and proteome expansion in metazoans. Nature 2002;418:236–43.

26. Proudfoot NJ, Furger A, Dye MJ. Integrating mRNA processing with transcription. Cell 2002;108:501–12.

27. Modrek B, Lee C. A genomic view of alternative splicing. Nat Genet 2002;30:13–9.

28. Caceres JF, Kornblihtt AR. Alternative splicing: multiple control mechanisms and involvement in human disease. Trends Genet 2002;18: 186–93.

29. Stoilov P, Meshorer E, Gencheva M, Glick D, Soreq H, Stamm S. Defects in Pre-mRNA Processing as Causes of and Predisposition to Diseases. DNA Cell Biol 2002;21:803–18.

30. Matsumura Y, Tarin D. Significance of CD44 gene products for cancer diagnosis and disease evaluation. Lancet 1992;340:1053–8.

31. Cannistra SA, Abu-Jawdeh G, Niloff J, et al. CD44 variant expression is a common feature of epithelial ovarian cancer: lack of association with standard prognostic factors. J Clin Oncol 1995;13:1912–21.

32. Stickeler E, Kittrell F, Medina D, Berget SM. Stage-specific changes in SR splicing factors and alternative splicing in mammary tumorigenesis. Oncogene 1999;18:3574–82.

33. Helfman DM, Roscigno RF, Mulligan GJ, Finn LA, Weber KS. Identification of two distinct intron elements involved in alternative splicing of beta-tropomyosin pre-mRNA. Genes Dev 1990;4:98–110.

34. Mulligan GJ, Guo W, Wormsley S, Helfman DM. Polypyrimidine tract binding protein interacts with sequences involved in alternative splicing of beta-tropomyosin pre-mRNA. J Biol Chem 1992;267: 25480–7.

35. Gooding C, Roberts GC, Smith CW. Role of an inhibitory pyrimidine element and polypyrimidine tract binding protein in repression of a regulated alpha-tropomyosin exon. Rna 1998;4:85–100.

36. Jin W, McCutcheon IE, Fuller GN, Huang ES, Cote GJ. Fibroblast growth factor receptor-1 alpha-exon exclusion and polypyrimidine tract-binding protein in glioblastoma multiforme tumors. Cancer Res 2000; 60:1221–4.

37. Carstens RP, Wagner EJ, Garcia-Blanco MA. An intronic splicing silencer causes skipping of the IIIb exon of fibroblast growth factor receptor 2 through involvement of polypyrimidine tract binding protein. Mol Cell Biol 2000;20:7388–400.

38. Le Guiner C, Plet A, Galiana D, et al. Polypyrimidine tract-binding protein represses splicing of a fibroblast growth factor receptor-2 gene alternative exon through exon sequences. J Biol Chem 2001;276: 43677–87.

39. Chan RC, Black DL. The polypyrimidine tract binding protein binds upstream of neural cell-specific c-src exon N1 to repress the splicing of the intron downstream. Mol Cell Biol 1997;17:4667–76.

40. Liu H, Zhang W, Reed RB, Liu W, Grabowski PJ. Mutations in RRM4 uncouple the splicing repression and RNA-binding activities of polypyrimidine tract binding protein. Rna 2002;8:137–49.

41. Norton PA. Polypyrimidine tract sequences direct selection of alternative branch sites and influence protein binding. Nucleic Acids Res 1994;22:3854–60.

42. Cote J, Dupuis S, Wu JY. Polypyrimidine track-binding protein binding downstream of caspase-2 alternative exon 9 represses its inclusion. J Biol Chem 2001;276:8535–43.

43. Southby J, Gooding C, Smith CW. Polypyrimidine tract binding protein functions as a repressor to regulate alternative splicing of alpha-actinin mutally exclusive exons. Mol Cell Biol 1999;19:2699–711.

44. Cartegni L, Chew SL, Krainer AR. Listening to silence and understanding nonsense: exonic mutations that affect splicing. Nat Rev Genet 2002;3:285–98.

45. Auersperg N, Maines-Bandiera SL, Dyck HG. Ovarian carcinogenesis and the biology of ovarian surface epithelium. J Cell Physiol 1997;173:261–5.